Water-Induced Reorganization of Ultrathin Nitrate Films on NaCl: Implications for the Tropospheric Chemistry of Sea Salt Particles

Heather C. Allen, J. M. Laux, Rainer Vogt, Barbara J. Finlayson-Pitts, and John C. Hemminger*

Department of Chemistry and Institute for Surface and Interface Science, University of California, Irvine, Irvine, California 92717

Received: December 11, 1995; In Final Form: February 5, 1996[⊗]

Reactions of sodium chloride, a major constituent of atmospheric sea salt particles which have been observed in the marine boundary layer as well as inland, and nitrogen oxides are known to form gas-phase chlorine species that may ultimately influence tropospheric ozone levels. Therefore, studies were carried out on sodium chloride single crystals which were exposed to nitric acid vapor at ∼298 K to form surface bonded nitrate. Upon exposure to water vapor pressures below the bulk dissolution (deliquescence) of sodium chloride and sodium nitrate, two-dimensional nitrate layers on the surface of sodium chloride crystals reorganized to form separate three-dimensional microcrystallites of sodium nitrate which were observed using transmission electron microscopy. X-ray photoelectron spectroscopy results show that the reorganization of the surface, and the regeneration of a fresh NaCl surface, also takes place under conditions where only 1−2 nitrate monolayers initially existed. These results explain atmospheric observations of highly variable chlorine deficits within individual sea salt particles and suggest that a large portion of the particle chloride, not just the original surface, may become available for reaction.

Introduction

Sodium chloride is the major constituent of sea salt particles which are generated by wave action and which constitute a substantial component of the particulates in the marine troposphere.[1−7] Thus, the reactions of solid NaCl with gaseous pollutants such as HNO_3, N_2O_5, NO_2, and $ClONO_2$ are potentially important because they produce sodium nitrate and gas-phase chlorinated products:[8−23]

$$HNO_3(g) + NaCl(s) \rightarrow NaNO_3(s) + HCl(g) \quad (1)$$

$$N_2O_5(g) + NaCl(s) \rightarrow NaNO_3(s) + ClNO_2(g) \quad (2)$$

$$2NO_2(g) + NaCl(s) \rightarrow NaNO_3(s) + ClNO(g) \quad (3)$$

$$ClONO_2(g) + NaCl(s) \rightarrow NaNO_3(s) + Cl_2(g) \quad (4)$$

The gas-phase products of reactions 2−4 are particularly significant since they will photolyze to form Cl atoms.[6,7,17] The subsequent reactions of atomic chlorine with O_3 or organics have the potential to play an important role in the determination of the tropospheric ozone concentrations.[24]

We have shown previously that the reaction of dry HNO_3 with solid NaCl(100) single crystals occurs with a reaction probability of 4×10^{-4} and is self-limiting.[25] That is, an ultrathin film (1−2 monolayers) of $NaNO_3$ is formed as the product and the reaction stops due to the formation of this "protective" film on the surface. Our recent infrared studies[19] also indicate that the environment of the nitrate species initially formed in the reactions of HNO_3 (or NO_2, or N_2O_5) with NaCl particles is altered by exposure to gas-phase water.

In this study we use transmission electron microscopy and X-ray photoelectron spectroscopy to show that exposure to water vapor of a NaCl crystallite which has been reacted with dry HNO_3 results in the recrystallization of the ultrathin nitrate layer to form small, three-dimensional sodium nitrate crystallites. This recrystallization process results in the exposure of fresh NaCl surface for further reaction. The result is that substantial fractions of the chlorine can be reacted from NaCl particles by reactions 1−4 in the presence of water vapor. Surprisingly, this recrystallization is observed to occur at water vapor relative humidities well below the deliquescence point of bulk NaCl(s) or $NaNO_3$(s).

Experimental Section

The reactions on NaCl were studied with X-ray photoelectron spectroscopy (XPS) and transmission electron microscopy-energy dispersive spectroscopy (TEM-EDS). The XPS experiments quantified the surface reaction of nitric acid with sodium chloride as a function of total dosage followed by exposure to water vapor. The TEM-EDS experiments identified changes in the morphology and composition of the sodium chloride surface after exposures to nitric acid and water vapor.

In the XPS experiments, an ESCALAB MKII photoelectron spectrometer (VG Scientific) with three separate ultrahigh vacuum (UHV) interconnected chambers (sample preparation, fast sample entry, and spectroscopy) was used. Typical background pressures were $(2-5) \times 10^{-10}$ Torr. The ESCALAB MKII is a multi-technique surface analysis instrument based on a UHV system. The XPS experiments were carried out in the spectroscopy chamber which is equipped with a standard Mg/Al twin anode X-ray source and a 150 mm radius hemispherical electron energy analyzer. Al Kα X-rays (1486.6 eV) were used in the experiments described here. All spectra were obtained using a constant analyzer pass energy of 20 eV.

NaCl(100) single crystals (Bicron) were used in the XPS experiments. After cleaving, the NaCl(100) crystals (5.0 mm × 5.0 mm × 1.0 mm) were clamped to a copper sample holder and then heated in UHV to 473 K to remove any impurities. XPS spectra confirmed the cleanliness of the NaCl surface to better than a few percent of a monolayer.

Nitric acid was prepared in a 50:50 v/v mixture with sulfuric

[⊗] Abstract published in *Advance ACS Abstracts,* March 15, 1996.

0022-3654/96/20100-6371$12.00/0

acid (Aldrich 70% A.C.S. reagent grade HNO_3 and Fisher 95−98% A.C.S. reagent grade H_2SO_4). In the XPS experiments, dosing of the NaCl sample with dry HNO_3 vapor above the HNO_3/H_2SO_4 mixture was carried out using an all glass capillary doser that was mounted on the sample preparation chamber and was thoroughly conditioned with dry HNO_3 prior to dosing the NaCl crystal. Details of the glass capillary doser apparatus have been published elsewhere.[25] Nitric acid pressures in the doser were measured by a Baratron capacitance manometer.

Water vapor exposure of the reacted sodium chloride crystal was carried out in the fast sample entry chamber by allowing water vapor to backfill into the chamber. (Transfer to and from interconnected chambers was carried out under UHV conditions.) A separate Baratron capacitance manometer was used to measure the water vapor pressures. The experimental arrangement allowed for rapid turn-on (1−5 s) and turn-off (∼10 s) of the water vapor exposures.

In the TEM-EDS experiments, most studies were performed at the UCI TEM facility in a Philips CM20 TEM (200kV) with an EDS attachment (EDAX PV9800) for detection of X-ray fluorescence. Magnification of the sample ranged between 22× and 660,000×. Typical magnification used to locate and view micron size crystals ranged between 200× and 50,000×. To limit electron beam damage, a Gatan Cold Stage (Model 636-P1) which cooled the samples to liquid nitrogen temperatures was used during EDS spectra acquisition. Local heating still occurred; however, the rate of heating of the sample was significantly inhibited, and therefore radiation damage was reduced.

For the TEM experiments, sodium chloride crystals were grown from a 0.2 M NaCl solution on the Formvar side of a Pelco Carbon-Type B nickel grid. Three small droplets of NaCl solution were initially placed on a Petri dish. Wiping of the grid over the droplets coalesced the drops underneath the Formvar coating. The grid was then allowed to "float" on top of the solution at ∼298 K until evaporation of the solution was complete (∼30 min). Cubic sodium chloride particles in the micron size range were obtained by periodic agitation during the crystallization process.

Exposure of the NaCl crystals to nitric acid vapor as a mixture in He was carried out inside an all-glass gas-handling manifold. Water vapor exposures were carried out by exposure either to laboratory relative humidity (RH) and/or to the equilibrium vapor pressure above a reservoir of deionized water. Inside the all-glass manifold, water vapor pressure was measured by two different Edwards high-vacuum pressure gauges (600AB transducer 1000 Torr range with a Model 1500 electronic manometer and a 570AB transducer 1000 Torr range with a Model 1174 electronic manometer). The 600AB transducer gauge has a manufacturer's stated accuracy of 0.15% and the 570AB transducer gauge 0.05% accuracy. The manifold relative humidity (RH) was calculated from the pressure measurements and the temperature. The laboratory relative humidity to which the sample was exposed (atmospheric water vapor) was recorded by a Fisher Scientific humidity/temperature meter (Digital Tachometer™, Model 11-88-6), calibrated against the National Institute of Standards and Technology Traceable Instrumentation with a limit of error of ±1.5% RH and ±0.4 °F. The calibration complies with the requirements of ISO 9000 Certification.

For light element EDS analysis (<Na), a Philips 420T TEM (120 kV) with a Kevex/Fisons Light Element EDS attachment (Sigma LPX2) at the University of Southern California Center for Electron Microscopy and Microanalysis (CEMMA) was utilized.

TEM-EDS Results

Figure 1a shows a typical cubic NaCl single crystal approximately 2.5 μm in size prior to reaction. After imaging, the NaCl crystals were transferred to the glass manifold and exposed to a flow of HNO_3 in helium ($[HNO_3] = 1.2 \times 10^{15}$ molecules cm^{-3} for 15 min). The HNO_3/He mixture was pumped off and followed by a flow of pure helium. The grid with the NaCl crystals was removed from the glass manifold and, in the process of transferring to the TEM, was exposed to laboratory air where the RH was measured to be 17% (4 Torr at 296 K). TEM images of the same crystals were then obtained (Figure 1b). At this resolution, there is no visible change in the morphology of the NaCl crystal. The grid was stored at a RH corresponding to water vapor pressures of 4−5 Torr at 295 K and the NaCl crystals were then exposed in the vacuum manifold to 15 Torr of water vapor (corresponding to a RH of 71%) for a few seconds and then 4 Torr (RH = 20%) for 2 min. The glass manifold was pumped and helium flowed through the reaction vessel for 1 min. The grid was transferred to the TEM at a maximum RH of 24%, corresponding to 5 Torr at 295 K. The images then obtained (Figure 1c) clearly show that the higher water vapor pressures induced a surface reorganization of the nitrate layer into separate microcrystallites of $NaNO_3$ on the NaCl crystal host. After imaging, the grid was removed and exposed to laboratory air at a RH of 22% (5 Torr at 296 K) and reacted a second time with HNO_3 ($[HNO_3] = 1.3 \times 10^{15}$ molecules cm^{-3} for 15 min) and then exposed to laboratory air at a RH of 24% (5 Torr at 297 K). A TEM image showed no visible change as compared to Figure 1c, and therefore this image is not shown here. TEM viewing was followed by 10.0−12.5 Torr water vapor exposure at 297 K (RH = 45%−56%). Figure 1d shows that after this second cycling of HNO_3 and then H_2O vapor, additional sodium nitrate crystallites attached to the NaCl were formed. EDS spectra confirmed the lack of chlorine in the newly formed crystallites (EDS detection at the UCI TEM facility is limited to heavy elements and is unable to detect the existence of nitrogen or oxygen).

Light-element energy dispersive spectroscopy was performed at the USC CEMMA facility on similarly reacted crystals for elemental identification to clarify the existence of $NaNO_3$ crystallites on the NaCl surface. Initially, the TEM electron beam was focused on a possible sodium nitrate crystallite on a corner of the sodium chloride host crystal. The spectrum in Figure 2a shows the nitrogen Kα peak at 0.392 keV, the oxygen Kα peak at 0.525 keV, the sodium Kα peak at 1.041 keV (and a small carbon Kα peak at 0.277 keV due to hydrocarbon contamination). This spectrum is very similar in relative element intensity to that of a sodium nitrate standard. The spectrum in Figure 2b was taken by focusing the TEM electron beam on the adjacent corner of the same reacted NaCl crystal. This corner appeared clean (no visible $NaNO_3$ growth). Clearly, no nitrogen or oxygen peak is present and only the Kα peak of sodium at 1.041 keV and the chloride peaks of Kα at 2.621 keV and Kβ at 2.815 keV were observed. When compared to other sodium chloride standards, this spectrum is very similar with respect to relative peak intensities. (Chlorine is a more efficient emitter of X-rays and therefore typically gives a much more intense EDS signal.) Conclusively, the light-element EDS spectra confirms $NaNO_3$ crystallite growth on the NaCl crystal host.

It is uncertain how much of the surface (i.e., to what depth) has reacted with nitric acid in these experiments. However, the XPS experiments described below confirm that the same

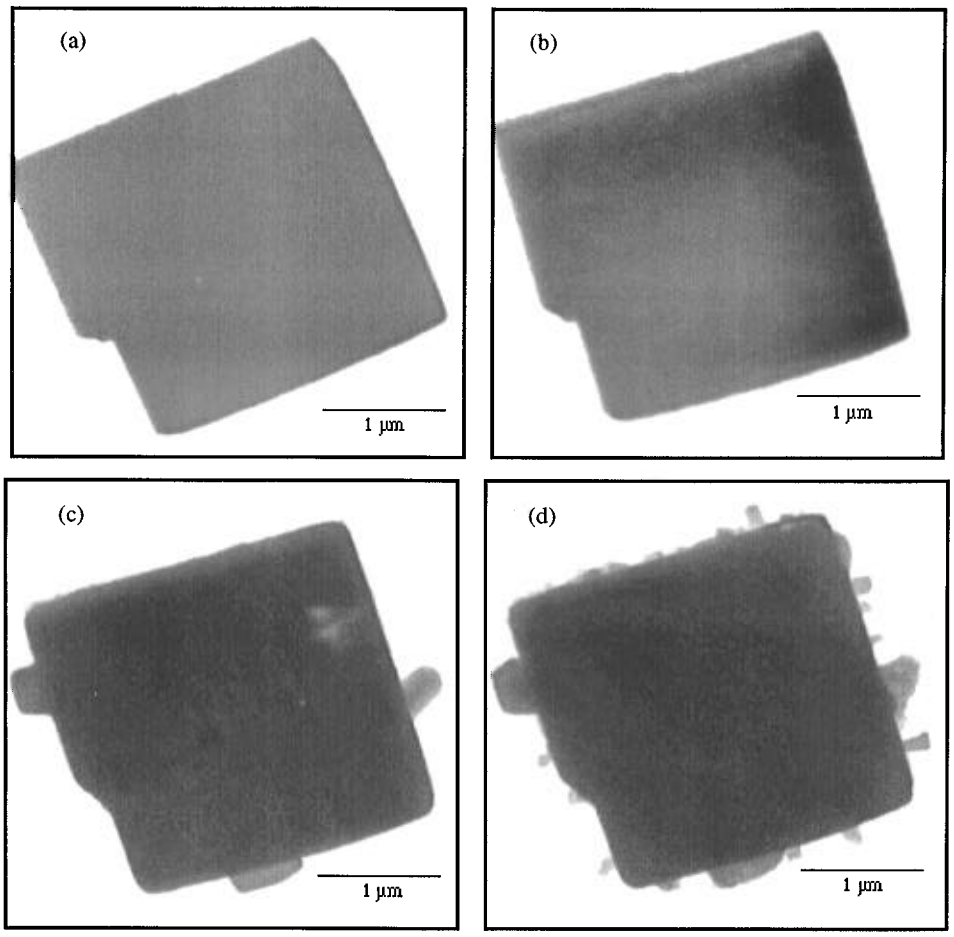

Figure 1. TEM micrographs of the same sodium chloride host crystal (a) before any exposure to HNO_3, (b) after exposure to HNO_3 (1.2×10^{15} molecules cm^{-3} for 15 min). (c) Following HNO_3 exposure, the crystal was exposed to water vapor pressure (<15 Torr), and (d) then exposed to another complete cycle consisting of HNO_3 (1.3×10^{15} molecules cm^{-3} for 15 min) followed by water vapor (<12.5 Torr).

phenomenon takes place under conditions where only 1−2 monolayers react.

XPS Results

Figure 3 shows a survey scan photoelectron spectrum of the NaCl surface following exposure of dry nitric acid to the sample. Nitrogen and oxygen are clearly observed as indicated by the N 1S peak at 407.8 eV and the O 1S peak at 533.3 eV (characteristic of a nitrate species). The binding energies reported here in the text are corrected for charging of the sample by assigning a binding energy of 1072.0 eV to the Na 1S peak. The sample charging observed in our experiments was only a few electronvolts in magnitude and quite constant from sample to sample. The figure inset shows the growth of the nitrogen 1S signal as a function of nitric acid exposure. Spectra such as these allow us to quantify the surface concentration of N, O, and Cl. Figure 4a shows the relative surface concentrations of N, O, and Cl as a function of nitric acid exposure, clearly indicating the saturation of the reaction after ∼20 min under the exposure conditions used in this experiment. The passivation of the surface is consistent with the formation of an unreactive ultrathin film of nitrate. The decrease in the Cl XPS signal can be used to estimate the thickness of the nitrate film. Assuming an attenuation length of 2.07 nm for Cl $2P_{3/2}$ electrons in the sodium nitrate layer,[43] the decrease in the Cl signal is consistent with a ∼1 nm thick nitrate film.

Figure 4b shows the effect of exposure to water vapor (3 Torr) of a surface which had been previously saturated with nitric acid. The observed decrease in the nitrogen signal and the increase in the chlorine signal is consistent with a three-dimensional recrystallization of the nitrate film, leaving freshly exposed NaCl surface. As three-dimensional crystallites of sodium nitrate are formed, a smaller fraction of the nitrate ions are near the surface to allow detection by XPS, leading to the decrease in N and O signals. At the same time, fresh NaCl is exposed leading to the observed increase in the Cl signal.

Discussion

Both the TEM and XPS results show that exposure to water vapor of sodium chloride crystals containing surface nitrate followed by removal of the water leads to phase separation of the chlorine and nitrate, with the concomitant growth of three-dimensional sodium nitrate crystallites. This recrystallization results in the generation of a clean surface of NaCl which is then available for further reaction. Perhaps most surprising, this phenomenon occurs at water vapor pressures below the deliquescence points of bulk sodium chloride (18.1 Torr at 298 K) or sodium nitrate (17.6 Torr at 298 K).[26]

Chung et al.[27] reacted NaCl with NO_2 and water vapor, and after further exposure to water vapor and drying, report sodium chloride and sodium nitrate diffraction patterns. However, no phase separation between the two crystalline structures appeared in their TEM micrographs even though water vapor exposure exceeded both sodium chloride and sodium nitrate deliquescence points. Although our results are qualitatively in agreement, we observe a separation of the sodium chloride and sodium nitrate crystals and in addition, the separation occurs below the deliquescence points.

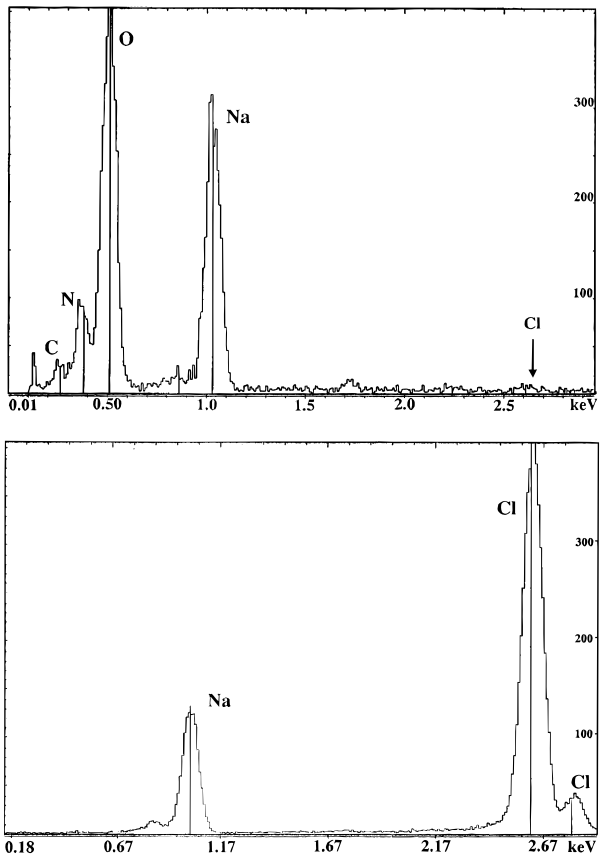

Figure 2. EDS light element spectra were acquired (a) from the $NaNO_3$ microcrystallites that had formed on the NaCl host crystal and (b) from an adjacent area of the NaCl host crystal.

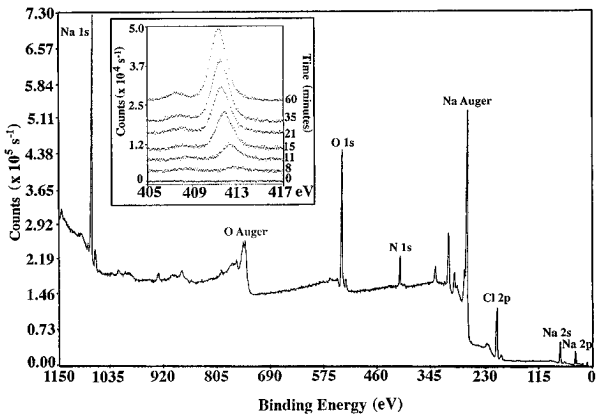

Figure 3. XPS survey scan spectrum of the NaCl surface following exposure to dry nitric acid. The inset shows the nitrogen 1S signal as a function of nitric acid exposure. Binding energies in this figure are not corrected for sample charging.

A number of studies in the past have documented the formation of interesting water structures on the surface of unreacted NaCl. For example, Barraclough and Hall[28] favor interpretation of their isotherm for H_2O on NaCl powders in terms of two-dimensional condensation of water on the solid surface. They also report that the salt behaved as if it had a liquid surface layer after adsorption of more than two water layers (corresponding to ~8−9 Torr), and proposed that this could lead to recrystallization of the surface, similar to what we observe for the reacted surface. Hucher et al.[29] followed changes in the surface conductivity of NaCl at 298 K and simultaneously changes in the surface structure as a function of water vapor pressure. They observed two domains below the deliquescence points. In the first, up to ~10 Torr water

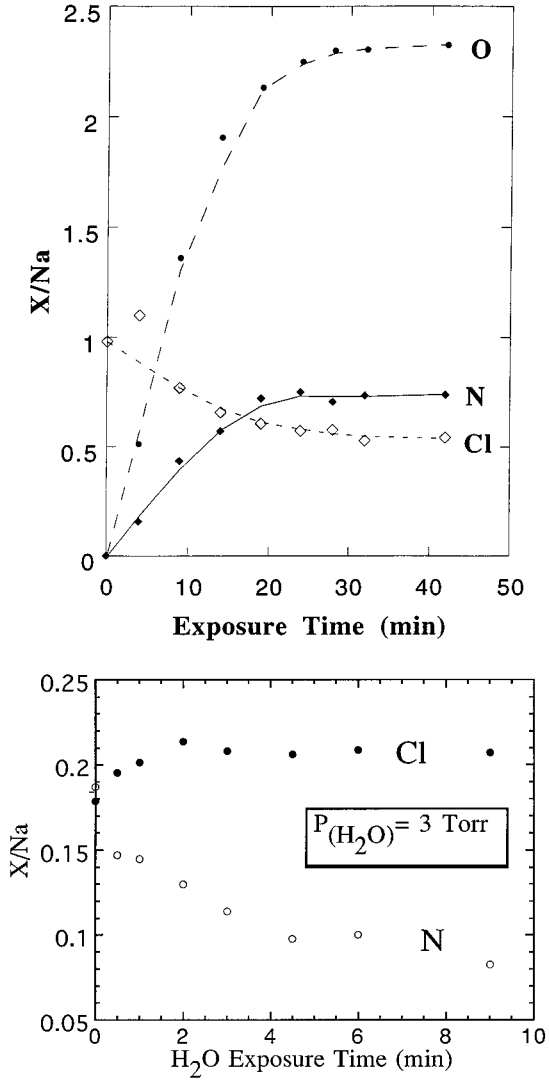

Figure 4. (a) XPS data from a NaCl (100) single crystal shows the relative surface concentrations of N, O, and Cl as a function of HNO_3-(g) exposure. Saturation is indicated after ~20 min of exposure time. (b) XPS data as a function of water vapor exposure (3 Torr) to the NaCl(100) surface following the HNO_3(g) exposure shows a decreasing N signal and an increasing Cl signal which indicates three-dimensional recrystallization of the ultrathin nitrate film.

vapor, physical adsorption of the water occurred, and between 10 Torr and the deliquescence point, cationic hydration with an associated relatively mobile phase on the surface was postulated. Similarly, molecular dynamics calculations and second harmonic generation experiments by Wasserman et al.[30] indicate that at low coverage, water adsorbs on polished NaCl windows as isolated molecules at cationic surface sites. However, at approximately half a monolayer coverage, a two-dimensional network of water molecules forms as the binding energy between water molecules exceeds that between water and the surface. Finally, Ewing and co-workers[31] observed that a two-dimensional water structure similar to a liquid forms on NaCl crystallites at 296 K at coverage corresponding to more than 20% of the surface sites.

A number of studies have shown that single crystal NaCl-(100) in UHV does not adsorb water (e.g., see Estel et al.[32]) at 298 K, which is confirmed by our lack of XPS observation of oxygen on our single crystals following exposure to only water. Adsorption of water on crystallites likely occurs initially at defects and edges. Prior reaction with HNO_3 disrupts the NaCl surface structure and generates an ultrathin nitrate film whose free energy is different from that of bulk sodium nitrate. This

surface may have a much larger number of effective defects and hence readily adsorb sufficient water to give a mobile network of two-dimensionally hydrogen bonded anions and cations. On pumping off the water, the formation of crystalline $NaNO_3$ ($\Delta H°_f = -111.8$ kJ mol^{-1}) and NaCl ($\Delta H°_f = -98.17$ kJ mol^{-1}) is thermodynamically favored over the surface-bonded nitrate species which is only bound in two, rather than three dimensions, as in the bulk crystal.

The present results are in agreement with our previous DRIFTS studies[19] in which we suggested the formation of a quasi-liquid layer on the salt surface under these conditions, similar to that proposed by Molina and co-workers on ice surfaces.[33] Such a quasi-liquid layer has also been implicated in the reaction of solid sodium sulfate with gaseous HCl, which proceeds readily in the presence of water vapor but not with the anhydrous salt.[34]

While sea salt particles will be in the form of concentrated solution droplets under many conditions in the marine boundary, there are a number of circumstances where relatively "dry" particles such as those studied here will exist. For example, in relatively dry coastal regions the relative humidity can be sufficiently low to dry out the droplets as the particles are transported away from the ocean surface. In addition, salt particles have been observed as far as 900 km inland[35] and were also found to be major components of plumes from oil well burning in Kuwait.[36-40]

TEM studies of the microscopic morphology of such particles show that marine particles are highly crystalline and exhibit phase separation of the chloride and nitrate components.[41,42] Our experiments show that these observations are consistent with the interaction of water vapor even at pressures below the deliquescence point with ultrathin films of nitrate, which is the initial reaction product on the salt surface, followed by phase separation and recrystallization.

This phenomenon appears to be quite general, occurring with salt surfaces prepared in different ways and observed using different techniques. Thus there is evidence for this water-induced reorganization of surface nitrate: (1) in micron-sized particles prepared by grinding and studied using DRIFTS;[19] (2) on small NaCl crystals formed by evaporation and studied using TEM-EDS; (3) on single crystals followed by XPS. This suggests that for a variety of prepared salt particles, surface nitrate will undergo reorganization and recrystallization into separate microcrystallites of $NaNO_3$, regenerating a fresh NaCl surface which is then available for further reaction. The reaction can continue to produce HCl until the chlorine in the sea salt particle is essentially depleted. This is consistent with the results of recent studies of particles in the marine boundary layer which established that some particles, particularly smaller ones, were largely depleted of chlorine.[4]

Summary

Our laboratory results show that while the reaction of dry nitric acid with NaCl is self-limiting due to the formation of a passivating nitrate film, water vapor induced recrystallization can lead to the selective recrystallization of the nitrate into microcrystallites of $NaNO_3$ and simultaneously to exposure of fresh sodium chloride for subsequent reaction. The fact that this can occur at vapor pressures below the bulk deliquescence point is the subject of ongoing studies in our laboratory.

Acknowledgment. We are grateful to the National Science Foundation (Grant No. ATM-9302475 and No. ATM-9222769), the Joan Irvine Smith and Athalie R. Clarke Foundation for support of this work, and Dr. P. Buseck , Dr. M. Posfai, and Dr. H. Sievering for sharing the results of their work prior to publication. We also thank Dr. M. Mecartney at the UCI TEM Facility for helpful comments, Dr. J. Worrall at the USC CEMMA, and T. Stark of Kevex/Fisons.

References and Notes

(1) Blanchard, D. C. *J. Geophys. Res.* **1985**, *90*, 961.
(2) Woodcock, A. H. *J. Meteorol.* **1953**, *10*, 362.
(3) Clegg, S. L.: Brimblecombe, P. *Atmos. Environ.* **1985**, *19*, 465.
(4) Mouri, H.; Okada, K. *Geophys. Res. Lett.* **1993**, *20*, 49.
(5) Cicerone, R. J. *Rev. Geophys. Space Phys.* **1981**, *19*, 123.
(6) Finlayson-Pitts, B. J. *Res. Chem. Int.* **1993**, *19*, 235.
(7) Graedel, T. E.; Keene, W. C. *Global Biogeochem. Cycles* **1995**, *9*, 47.
(8) Robbins, R. C.; Cadle, R. D.; Eckhardt, D. L. *J. Meteorol.* **1959**, *16*, 53.
(9) Cadle, R. D.; Robbins, R. C. *Discuss. Faraday Soc.* **1960**, *30*, 155.
(10) Leu, M. T.; Timonen, R. S.; Keyser, L. F.; Yung, Y. L. *J. Phys. Chem.* **1995**, *99*, 13203.
(11) Fenter, F. F.; Caloz, F.; Rossi, M. J. *J. Phys. Chem.* **1994**, *98*, 9801.
(12) Finlayson-Pitts, B. J.; Ezell, M. J.; Pitts, J. N., Jr. *Nature* **1989**, *337*, 241.
(13) Livingston, F. E.; Finlayson-Pitts, B. J. *Geophys. Res. Lett.* **1989**, *18*, 17.
(14) Behnke, W.; Scheer, V.; Zetzsch, C. *J. Aerosol Sci.* **1993**, *24*, S115.
(15) George, Ch.; Ponche, J. L.; Mirabel, Ph.; Behnke, W.; Scheer, V.; Zetzsch, C. *J. Phys. Chem.* **1994**, *98*, 8780.
(16) Msibi, I. M.; Li, Y.; Shi, J. P.; Harrison, R. M. *J. Atmos. Chem.* **1994**, *18*, 291.
(17) Schroeder, W. H.; Urone, P. *Environ. Sci. Technol.* **1974**, *8* , 756.
(18) Finlayson-Pitts, B. J. *Nature* **1983**, *306*, 676.
(19) Vogt, R.; Finlayson-Pitts, B. J. *J. Phys. Chem.* **1994**, *98*, 3747; **1995**, *99*, 13052.
(20) Vogt, R.; Finlayson-Pitts, B. J. *Geophys. Res. Lett*. **1994**, *21*, 2291.
(21) Junkermann, W.; Ibusuki, T. *Atmos. Environ.* **1992**, *26A*, 3099.
(22) Winkler, T.; Goschnick, J.; Ache, H. J. *J. Aerosol Sci.* **1991**, *22*, S605.
(23) Timonen, R. S.; Chu, L. T.; Leu, M. T.; Keyser, L. F. *J. Phys. Chem.* **1994**, *98*, 9509.
(24) Finlayson-Pitts, B. J.; Pitts, J. N., Jr. *Atmospheric Chemistry: Fundamentals and Experimental Techniques*; John Wiley and Sons: New York, 1986.
(25) Laux, J. M.; Hemminger, J. C.; Finlayson-Pitts, B. J. *Geophys Res. Lett.* **1994**, *21*, 1623.
(26) Pilinis, C.; Seinfeld, J. H.; Grosjean, D. *Atmos. Environ.* **1989**, *23*, 1601.
(27) Chung, T. T.; Dash, J.; O'Brien, R. J. *9th Int. Cong. Electron Microsc.* **1978**, *1*, 440.
(28) Barraclough, P. B.; Hall, P. G. *Surf. Sci.* **1974**, *46*, 393.
(29) Hucher, M.; Oberlin, A.; Hocart, *R. Bull. Soc. Fr. Mineral. Crist.* **1967**, *90*, 320.
(30) Wassermann, B.; Mirbt, S.; Reif, J.; Zink, J. C.; Matthias, E. *J. Chem. Phys.* **1993**, *98*, 10049.
(31) Dai, D. J.; Peters, S. J.; Ewing, G. E. *J. Phys. Chem.* **1995**, *99*, 10299.
(32) Estel, J.; Hoinkes, H.; Kaarmann, H.; Nahr, H.; Wilsch, H. *Surf. Sci.* **1976**, *54*, 393.
(33) Abbatt, J. P. D.; Beyer, K. D.: Fucaloro, A. F.; McMahon, J. R.; Wooldridge, P. J.; Zhang, R.; Molina, M. *J. Geophys. Res.* **1992**, *97*, 15819.
(34) Benson, S. W.; Richardson, R. L. *J. Am. Chem. Soc.* **1955**, *77*, 4206.
(35) Shaw, G. E. *J. Geophys. Res.* **1991**, *96*, 22369.
(36) Lowenthal, D. H.; Borys, R. D.; Rogers, C. F.; Chow, J. C.; Stevens, R. K.; Pinto, J. P.; Ondov, J. M. *Geophys. Res. Lett.* **1993**, *20*, 691.
(37) Stevens, R.; Pinto, J.; Mamane, Y.; Ondov, J.; Abdulraheem, M.; Al-Majed, N.; Sadek, M.; Cofer, W.; Ellenson, W.; Kellog, R. *Water Sci. Technol.* **1993**, *27*, 223.
(38) Sheridan, P. J.; Schnell, R. C.; Hofmann, D. J.; Harris, J. M.; Deshler, T. *Geophys. Res. Lett.* **1992**, *19*, 389.
(39) Parungo, F.; Kopcewicz, B.; Nagamoto, C.; Schnell, R.; Sheridan, P.; Zhu, C.; Harris, J. *J. Geophys. Res.* **1992**, *97*, 15867.
(40) Cahill, T. A.; Wilkinson, K.; Schnell, R. *J. Geophys. Res.* **1992**, *97*, 14513.
(41) Posfai, M.; Anderson, J. R.; Buseck, P. R.; Shattuck, T. W.; Tindale, N. W. *Atmos. Environ.* **1994**, *28*, 1747.
(42) Posfai, M.; Anderson, J. R.; Buseck, P. R.; Sievering, H. *J. Geophys. Res.* **1995**, *100*, 23063.
(43) Briggs, S.; Seah, M. P. *Practical Surface Analysis*, 2nd ed.; John Wiley and Sons: New York, 1990.

JP953675A